ZU-TH 07/08
SLAC-PUB-13263

Two-Loop Fermionic Corrections to Heavy-Quark Pair Production: the Quark-Antiquark Channel

R. Bonciani [a,*], **A. Ferroglia** [a,†], **T. Gehrmann** [a,‡], **D. Maître** [b,§] **and C. Studerus** [a,¶]

[a] *Institut für Theoretische Physik, Universität Zürich, CH-8057 Zurich, Switzerland*

[b] *Stanford Linear Accelerator Center, Stanford University, Stanford, CA 94390, USA*

Abstract: We evaluate the fermionic two-loop QCD corrections to the heavy-quark pair production process in the quark-antiquark channel. We obtain analytic results which are valid for any value of the Mandelstam invariants s and t, and of the heavy quark mass m. Our findings confirm previous results for the analytic evaluation in the small-mass limit and numerical results for the exact amplitude. We furthermore provide the expansion of the two-loop amplitude at the production threshold $s \gtrsim 4m^2$.

Keywords: Heavy Quark Production, Two Loop Calculation.

*Email: Roberto.Bonciani@physik.uzh.ch
†Email: Andrea.Ferroglia@physik.uzh.ch
‡Email: Thomas.Gehrmann@physik.uzh.ch
§Email: maitreda@slac.stanford.edu
¶Email: cedric@physik.uzh.ch

Published in the Journal of High Energy Physics (JHEP)
Work supported in part by US Department of Energy contract DE-AC02-76SF00515

Contents

1. Introduction

The top quark is the heaviest fermion of the Standard Model. By studying its properties in detail, it is hoped to elucidate the origin of particle masses and the mechanism of electroweak symmetry breaking. Since its discovery at the Fermilab Tevatron [1] a little more than a decade ago, its mass has been measured to within a few per cent, while its production cross section and couplings are only known with larger uncertainty. With the large number of top quarks expected to be produced at the LHC, the study of its properties will become precision physics. To interpret these upcoming precision data, equally precise theoretical predictions are mandatory. These demand foremost the calculation of higher order corrections in perturbative QCD.

At present, the top quark pair production cross section [2–8] is known to next-to-leading order (NLO) in the QCD coupling constant, the same precision is available for single top production [9], $t\bar{t}$+jet production [10] and $t\bar{t}$+Z-boson production [11]. For the pair production cross section, resummation [12–14] of logarithmically enhanced corrections (next-to-leading logarithm, NLL) to all orders in the coupling constant improves upon the fixed-order NLO prediction. Electroweak one-loop corrections to $t\bar{t}$ production are equally available [15, 16].

Especially for the top quark pair production cross section, which is expected to be measured to within a few per cent accuracy, it is believed that the current NLO+NLL prediction is not yet sufficiently accurate. Detailed recent studies [17–19] indicate a scale uncertainty on these predictions of 7%, and a parton distribution uncertainty of 6%. While the latter

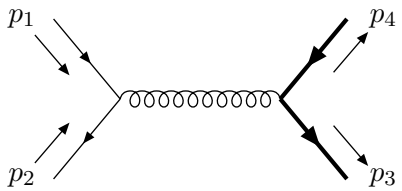

Figure 1: *Tree-level amplitude. Massive quarks are indicated by a thick line.*

may be improved upon by more precise determinations of the parton distribution functions in view of recent and upcoming data from HERA and LHC, the former requires the calculation of perturbative corrections at next-to-next-to-leading order (NNLO) in QCD. By approximating these corrections with the fixed-order expansion of the NLL prediction, one finds [17] a projected NNLO scale uncertainty of 3%, which is below the parton distribution uncertainty, and in line with the anticipated experimental error.

The calculation of the full NNLO corrections to the top quark pair production cross section requires three types of ingredients: two-loop matrix elements for $q\bar{q} \to t\bar{t}$ and $gg \to t\bar{t}$, one-loop matrix elements for hadronic production of $t\bar{t}$+(1 parton) and tree-level matrix elements for hadronic production of $t\bar{t}$+(2 partons). The latter two ingredients were computed previously in the context of the NLO corrections to $t\bar{t}$+jet production [10]. They contribute to the $t\bar{t}$ production cross section through configurations where up to two final state partons can be unresolved (collinear or soft), and their implementation thus may require further developments of subtraction techniques at NNLO.

Both two-loop matrix elements were computed analytically in the small-mass expansion limit $s, |t|, |u| \gg m^2$ in [20,21], starting from the previously known massless two-loop matrix elements for $q\bar{q} \to q'\bar{q}'$ [22] and $gg \to q\bar{q}$ [23]. An exact numerical representation of the two-loop matrix element $q\bar{q} \to t\bar{t}$ has been obtained very recently [24]. It is the aim of the present paper to compute all two-loop contributions to $q\bar{q} \to t\bar{t}$ arising from closed fermion loops in a compact analytic form, which provide a first independent validation of the recent results of [20, 24], allow for a fast numerical evaluation, and permit the analytical study of the behavior of the top quark production cross section at threshold.

This paper is structured as follows. In Section 2, we define our notation and kinematical conventions. Sections 3 and 4 describe the details of the calculation of the two-loop integrals and of the renormalization of the amplitudes. The results are presented and discussed in Section 5. We enclose two appendices describing the special functions used in our calculation and documenting the newly computed master integrals.

2. Notation and Conventions

We consider the scattering process

$$q(p_1) + \overline{q}(p_2) \longrightarrow t(p_3) + \overline{t}(p_4)\,, \tag{2.1}$$

in Euclidean kinematics, where $p_i^2 = 0$ for $i = 1, 2$ and $p_j^2 = -m^2$ for $i = 3, 4$. The Mandelstam variables are defined as follows

$$s = -(p_1 + p_2)^2 , \quad t = -(p_1 - p_3)^2 , \quad u = -(p_1 - p_4)^2 . \tag{2.2}$$

Conservation of momentum implies that $s + t + u = 2m^2$.

The squared tree-level matrix element (averaged over the spin and color of the incoming quarks and summed over the spin of the outgoing ones), calculated in $d = 4-2\varepsilon$ dimensions, can be expanded in powers of the strong coupling constant α_S as follows:

$$|\mathcal{M}|^2(s, t, m, \varepsilon) = \frac{4\pi^2\alpha_S^2}{N_c^2}\left[\mathcal{A}_0 + \left(\frac{\alpha_s}{\pi}\right)\mathcal{A}_1 + \left(\frac{\alpha_s}{\pi}\right)^2\mathcal{A}_2 + \mathcal{O}\left(\alpha_s^3\right)\right] . \tag{2.3}$$

The tree-level amplitude involves a single diagram (Fig. 1) and its contribution to Eq. (2.3) is given by

$$\mathcal{A}_0 = 4N_c\, C_F\left[\frac{(t-m^2)^2 + (u-m^2)^2}{s^2} + \frac{2m^2}{s} - \varepsilon\right] , \tag{2.4}$$

where N_c is the number of colors and $C_F = (N_c^2 - 1)/2N_c$. As it is well known, the term proportional to the dimensional regulator ε in Eq. (2.4) is mass independent.

The NLO term $\mathcal{A}_1$ in Eq. (2.3) arises from the interference of one-loop diagrams with the tree-level amplitude [2–8]. The NNLO term $\mathcal{A}_2$ consists of two parts, the interference of two-loop diagrams with the Born amplitude and the interference of one-loop diagrams among themselves:

$$\mathcal{A}_2 = \mathcal{A}_2^{(2\times0)} + \mathcal{A}_2^{(1\times1)} .$$

The latter term $\mathcal{A}_2^{(1\times1)}$ was studied extensively in [25]. $\mathcal{A}_2^{(2\times0)}$, originating from the two-loop diagrams, can be decomposed according to color and flavor structures as follows:

$$\begin{aligned}\mathcal{A}_2^{(2\times0)} = N_c C_F\Bigg[&N_c^2 A + B + \frac{C}{N_c^2} + N_l\left(N_c D_l + \frac{E_l}{N_c}\right) + N_h\left(N_c D_l + \frac{E_l}{N_c}\right)\\ &+ N_l^2 F_l + N_l N_h F_{lh} + N_h^2 F_h\Bigg] ,\end{aligned} \tag{2.5}$$

where N_l and N_h are the number of light- and heavy-quark flavors, respectively. The coefficients $A, B, \ldots, F_h$ in Eq. (2.5) are functions of s, t, and m, as well as of the dimensional regulator ε. Recently, these quantities were calculated in [20] in the approximation $s, |t|, |u| \gg m^2$. For a fully differential description of top quark pair production at NNLO, the complete mass dependence of $\mathcal{A}_2^{(2\times0)}$ is required. An exact numerical expression for it has been obtained very recently in [24]. In this work, we provide independent confirmations of the recent results of [20, 24] by deriving exact analytic expressions for all the terms in Eq. (2.5) arising from two-loop diagrams involving at least a fermion loop (i.e. the coefficients D_i, E_i, F_j with $i = l, h$ and $j = l, h, lh$).

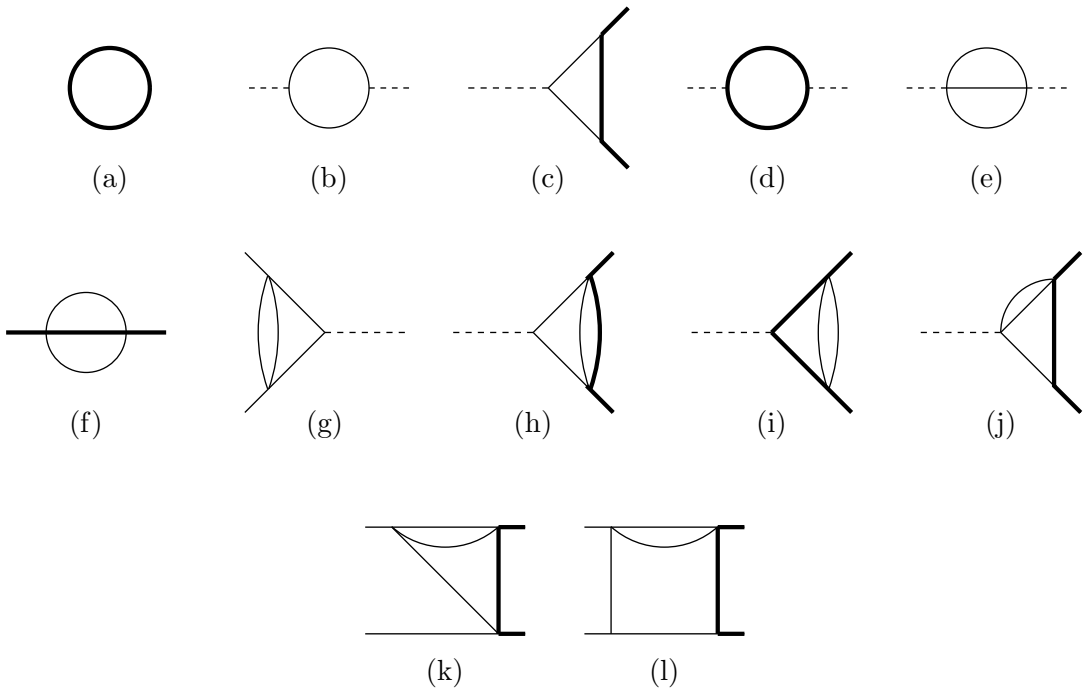

Figure 2: *Non-reducible topologies for the light quark corrections.*

3. Calculation

The calculation starts from the two-loop Feynman diagrams for $q\bar{q} \to t\bar{t}$, which are generated using QGRAF [26], interfered with the tree-level amplitude, and simplified using FORM [27]. Out of the 218 two-loop diagrams contributing to the amplitude, 28 are proportional to N_l, 29 are proportional to N_h, 2 are proportional to $N_l N_h$, while just one contributes to the N_l^2 and N_h^2 parts. Most importantly, there is only one two-loop box topology contributing to the N_l part of the squared amplitude, and a single other two-loop box topology proportional to N_h. These two box topologies are very similar to the ones encountered in the evaluation of the two-loop QED corrections to Bhabha scattering [28,29], and can be evaluated with the same techniques.

All two-loop integrals appearing in these amplitudes are reduced to a set of master integrals (MIs) by means of the standard method based on the Laporta algorithm [30]. Only part of these MIs were available in the literature [31–37] from previous two-loop calculations of the heavy quark form factors [38] and amplitudes for Bhabha scattering [28,29,39]. For the remaining integrals, we employed the differential equation method [40].

The reduction to MIs was carried out with two independent implementations of the Laporta algorithm, and large parts of it were cross checked with the `Maple` package `A.I.R.` [41]. The 12 irreducible topologies encountered in the calculation of the diagrams with a light quark loop are shown in Fig. 2. The diagrams proportional to N_h also contain 12 irreducible topologies, which can be found in Fig. 3. In both figures, thick internal lines indicate massive propagators, while thin lines indicate massless ones. An external

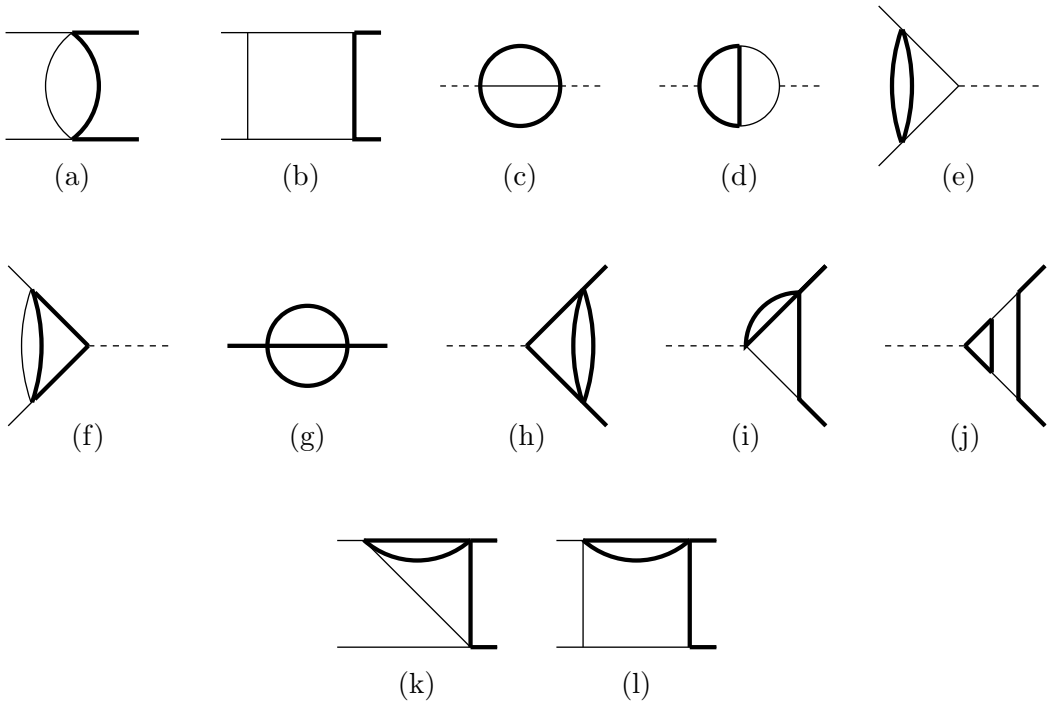

Figure 3: *Non-reducible topologies for the heavy quark corrections.*

dashed leg carries a squared momentum s; other external lines indicate particles on their mass-shell, where $p_i^2 = 0$ for thin lines and $p_i^2 = -m^2$ for thick lines.

The analytic expressions of the one-loop MIs in Fig. 2 and Fig. 3 are well known. The large majority of the two-loop MIs is also known in the literature: explicit analytic expressions for all the two-loop MIs with the exception of the ones belonging to topologies Fig. 2-(k), Fig. 2-(l), Fig. 3-(k), and Fig. 3-(l) can be found in [31–33, 35].

The MIs associated with topologies Fig. 2-(k), Fig. 2-(l), Fig. 3-(k), and Fig. 3-(l) that were not available in the literature are collected in Appendix B. In calculating the MIs by means of the differential equation method, it is crucial to fix the undetermined integration constant(s) appearing in the solution of the differential equations. While there is no general method available to fix such initial condition, it is usually sufficient to know the behavior of the MI in some particular kinematic point; for example, knowing that the integral is regular for a certain value of s, one can impose the regularity of the solution of the differential equation in that point. This can be sufficient to determine the integration constant. In our calculation, the initial conditions for the single master integral belonging to topology Fig. 2-(k) and the two MIs belonging to topology Fig. 3-(l) were determined by imposing the regularity of the solution of the differential equation in $t = 0$. However, this is not always sufficient. For topology Fig. 3-(k), which has two MIs, imposing the regularity of both MIs in $t = 0$ allowed to fix only one of the two initial conditions required. In order to fix the second integration constant, we had to use another piece of information, namely that the scalar integral with all the denominators raised to power one diverges

at most logarithmically at the threshold $t = m^2$. The final result for these two MIs was then checked by calculating their $t \to 0$ limit with the Mellin Barnes technique, using the `Mathematica` packages `Ambre` [42] and `MB` [43]. For what concerns the MI of the box topology in Fig. 2-(l), the initial conditions were defined calculating the integral in $t = 0$ with Mellin Barnes techniques.

All the MIs were calculated in the non-physical region $s < 0$, where they are real and can be conveniently written as functions of the dimensionless variables

$$x = \frac{\sqrt{-s+4m^2} - \sqrt{-s}}{\sqrt{-s+4m^2} + \sqrt{-s}}\,, \qquad y = \frac{-t}{m^2}\,, \qquad z = \frac{-u}{m^2}\,. \tag{3.1}$$

The MIs of the topology Fig. 3-(e) are an exception. In this case it is convenient to employ the variable

$$x_p = \frac{\sqrt{-s} - \sqrt{-s-4m^2}}{\sqrt{-s} + \sqrt{-s-4m^2}}\,. \tag{3.2}$$

The transcendental functions appearing in the MIs are one- and two-dimensional harmonic polylogarithms (HPLs) [44, 45]. In the result one finds one-dimensional HPLs of maximum weight four and two-dimensional HPLs of maximum weight three. Both sets of functions can be rewritten in terms of conventional Nielsen's polylogarithms. In Appendix A, we briefly review the definition of the HPLs employed and we collect the expression of some of them in terms of Nielsen's polylogarithms.

Following the procedure outlined in the present section, it is possible to obtain the expression of the bare squared matrix elements involving diagrams proportional to N_l and/or N_h. After this goal is achieved, it is then necessary to renormalize the ultraviolet divergencies. In the next section, we briefly discuss the renormalization procedure and we explicitly list the needed renormalization constants.

4. Renormalization

The renormalized QCD matrix element is obtained from the bare one by expanding the following expression :

$$\mathcal{A}_{\rm ren} = \prod_n Z_{{\rm WF},n}^{1/2}\, \mathcal{A}_{\rm bare}\left(\alpha_{S,{\rm bare}} \to Z_{\alpha_S}\alpha_S\,, m_{\rm bare} \to Z_m m\right)\,, \tag{4.1}$$

where $Z_{{\rm WF},n}$ is the external leg wave function renormalization factor, α_S is the renormalized coupling constant and m is the renormalized heavy quark mass. (In the rest of the section we suppress the subscript "S" in α_S).

We postpone the discussion of mass renormalization to the end of the section and we start by considering the coupling constant and wave function renormalization.

We introduce the following quantities:

$$a_0 = \frac{\alpha_{\rm bare}}{\pi}\,, \qquad \text{and} \qquad a = \frac{\alpha}{\pi}\,. \tag{4.2}$$

By expanding the amplitude and the wave function renormalization factor in a_0 we find:

$$\begin{aligned} \mathcal{A}_{\rm ren}(\alpha_{\rm bare}) &= a_0\mathcal{A}_0 + a_0^2\mathcal{A}_1 + a_0^3\mathcal{A}_2 + \mathcal{O}(a_0^4)\,, \\ Z_{{\rm WF},n} &= 1 + a_0\delta Z_{{\rm WF},n}^{(1)} + a_0^2\delta Z_{{\rm WF},n}^{(2)} + \mathcal{O}(a_0^3)\,. \end{aligned} \tag{4.3}$$

The relation between a_0 and a is given by:

$$a_0 = a + a^2 \delta Z_\alpha^{(1)} + a^3 \delta Z_\alpha^{(2)} + \mathcal{O}(a^4)\,. \tag{4.4}$$

By employing Eqs. (4.3,4.4) in Eq. (4.1) we find

$$\begin{aligned}
\mathcal{A}_{\rm ren} &= a\mathcal{A}_0 + a^2 \mathcal{A}_{\rm ren}^{(1)} + a^3 \mathcal{A}_{\rm ren}^{(2)} + \mathcal{O}(a^4)\,,\\
\mathcal{A}_{\rm ren}^{(1)} &= \mathcal{A}_1 + \left(\sum_n \frac{1}{2} \delta Z_{{\rm WF},n}^{(1)} + \delta Z_\alpha^{(1)} \right) \mathcal{A}_0\,,\\
\mathcal{A}_{\rm ren}^{(2)} &= \mathcal{A}_2 + \left(\sum_n \frac{1}{2} \delta Z_{{\rm WF},n}^{(1)} + 2\delta Z_\alpha^{(1)} \right) \mathcal{A}_1 + \left(-\sum_n \frac{1}{8} \left(\delta Z_{{\rm WF},n}^{(1)} \right)^2 \right.\\
&\quad \left. + \sum_n \frac{1}{2} \delta Z_{{\rm WF},n}^{(2)} + \delta Z_\alpha^{(1)} \sum_n \delta Z_{{\rm WF},n}^{(1)} + \delta Z_\alpha^{(2)} \right) \mathcal{A}_0\,.
\end{aligned} \tag{4.5}$$

In the equations above, $\mathcal{A}_i$ represents the amplitude at i loops stripped of the factor a. In the case of the process $q\overline{q} \to t\overline{t}$, the wave function renormalization factors of massless quarks vanish at one loop, while the ones of the massive quarks in the on-shell renormalization scheme are given by

$$\delta Z_{{\rm WF},M}^{(1)} = C(\varepsilon) \left(\frac{\mu^2}{m^2} \right)^\varepsilon C_F \left(-\frac{3}{4\varepsilon} - \frac{1}{1-2\varepsilon} \right)\,, \tag{4.6}$$

where the subscript M indicates massive quarks and where $C(\varepsilon) = (4\pi)^\varepsilon \Gamma(1+\varepsilon)$. The one-loop renormalization constant for α in the $\overline{MS}$ scheme is given by

$$\delta Z_\alpha^{(1)} = C(\varepsilon) \frac{e^{-\gamma\varepsilon}}{\Gamma(1+\varepsilon)} \left(-\frac{\beta_0}{2\varepsilon} \right)\,, \tag{4.7}$$

where $\beta_0 = 11/6 C_A - 1/3(N_l + N_h)$ and γ is the Euler-Mascheroni constant $\gamma \approx 0.577216$.

Therefore, the overall one-loop counter term is given by

$$\delta Z_{{\rm WF},M}^{(1)} + \delta Z_\alpha^{(1)} = -\frac{C(\varepsilon)}{4\varepsilon} \left[2\beta_0 + 3 + 4\varepsilon + \ln\left(\frac{\mu^2}{m^2} \right) \right] + \mathcal{O}\left(\varepsilon^2\right)\,. \tag{4.8}$$

To renormalize the two-loop diagrams contributing to the N_l corrections of the partonic cross section it is necessary to extract from the last two lines in Eq. (4.5) the terms proportional to N_l. Taking into account the fact that the wave function renormalization factors are zero for the incoming particles and identical for the massive ones, we find that

$$\begin{aligned}
\mathcal{A}_{\rm ren}^{(2,N_l)} &= \mathcal{A}_2^{(N_l)} + \left(\delta Z_{{\rm WF},M}^{(1)} + 2\delta Z_\alpha^{(1,C_A)} \right) \mathcal{A}_1^{(d_1)} + 2\delta Z_\alpha^{(1,N_l)} \sum_{j=3}^{10} \mathcal{A}_1^{(d_j)}\\
&\quad + \left(\delta Z_{{\rm WF},M}^{(2,N_l)} + 2\delta Z_\alpha^{(1,N_l)} \delta Z_{{\rm WF},M}^{(1)} + \delta Z_\alpha^{(2,N_l)} \right) \mathcal{A}_0\,.
\end{aligned} \tag{4.9}$$

In Eq. (4.9), the quantity $\mathcal{A}_1^{(d_j)}$ is the amplitude of the j-th diagram in Fig. 4 (stripped of the factor a). The renormalization coefficients not previously defined are:

$$\delta Z_\alpha^{(1,N_l)} = C(\varepsilon) \frac{e^{-\gamma\varepsilon}}{\Gamma(1+\varepsilon)} \frac{N_l}{6\varepsilon}\,,$$

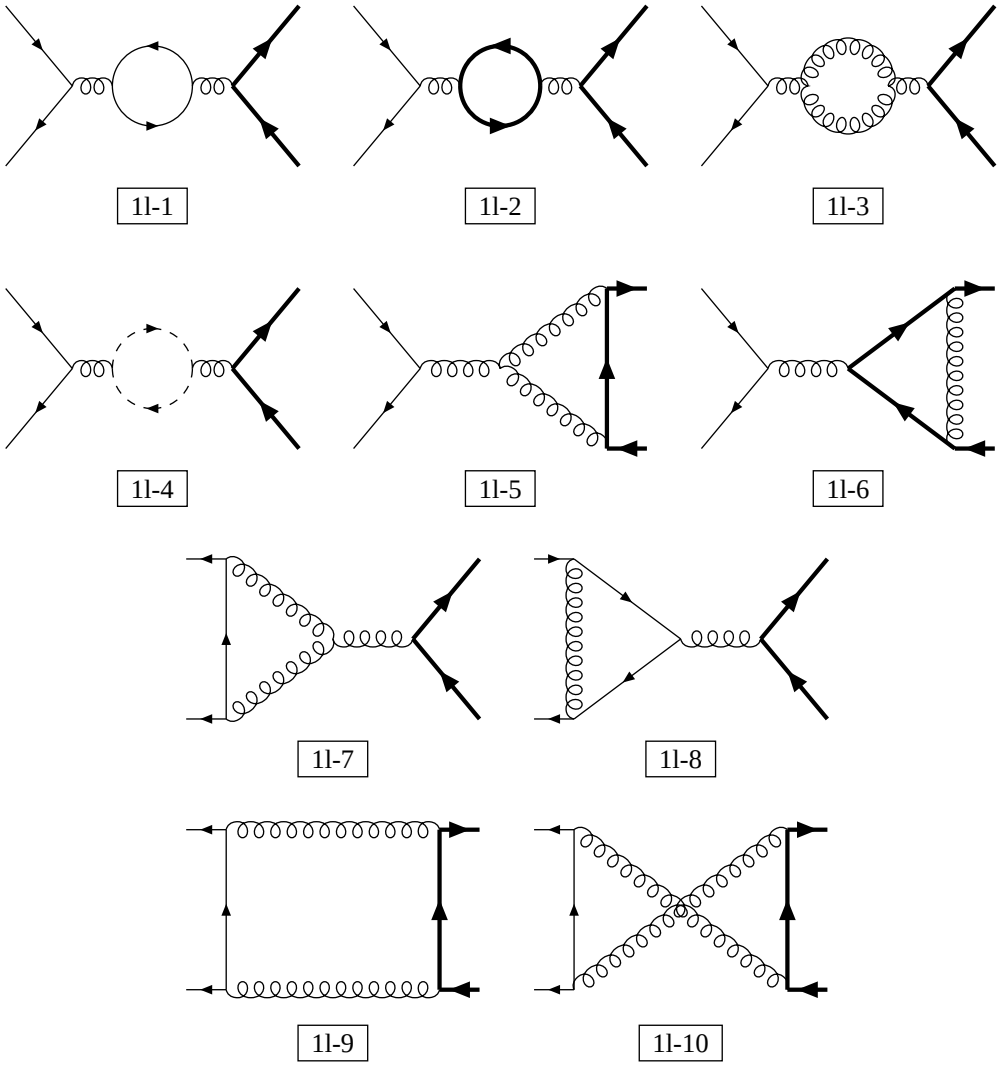

Figure 4: *One-loop diagrams. Thin arrow lines represent massless quarks, thick arrow line massive quarks, dashed arrow lines are Faddeev-Popov ghosts, and coiled lines are gluons.*

$$
\begin{aligned}
\delta Z_\alpha^{(1,C_A)} &= -C(\varepsilon)\,\frac{e^{-\gamma\varepsilon}}{\Gamma(1+\varepsilon)}\,C_A\frac{11}{12\varepsilon}\,,\\
\delta Z_\alpha^{(2,N_l)} &= C(\varepsilon)^2\,\left(\frac{e^{-\gamma\varepsilon}}{\Gamma(1+\varepsilon)}\right)^2\frac{N_l}{4\varepsilon}\left(\frac{5}{12}C_A+\frac{1}{4}C_F-\frac{11}{9\varepsilon}C_A\right)\,,\\
\delta Z_{\mathrm{WF},M}^{(2,N_l)} &= C(\varepsilon)^2\left(\frac{\mu^2}{m^2}\right)^{2\varepsilon}C_F N_l\left(\frac{1}{16\varepsilon^2}+\frac{9}{32\varepsilon}+\frac{59}{64}+\frac{\pi^2}{24}+\mathcal{O}\left(\varepsilon\right)\right)\,. \qquad (4.10)
\end{aligned}
$$

In order to renormalize the part of the squared matrix element proportional to N_h, one has to consider the terms proportional to N_h in the last two lines of Eq. (4.5), and to add the counter term for the on-shell mass renormalization:

$$
\mathcal{A}_{\mathrm{ren}}^{(2,N_h)}=\mathcal{A}_2^{(N_h)}+\left(\delta Z_{\mathrm{WF},M}^{(1)}+2\delta Z_\alpha^{(1,C_A)}\right)\mathcal{A}_1^{(d_2)}+2\delta Z_\alpha^{(1,N_h)}\sum_{j=3}^{10}\mathcal{A}_1^{(d_j)}-2\delta Z_m^{(1)}\mathcal{A}_1^{(d_2,\texttt{mass CT})}
$$

$$+\left(\delta Z_{\mathrm{WF},M}^{(2,N_h)}+\delta Z_{\mathrm{WF},m}^{(2,N_h)}+2\delta Z_{\alpha}^{(1,N_h)}\delta Z_{\mathrm{WF},M}^{(1)}+\delta Z_{\alpha}^{(2,N_h)}\right)\mathcal{A}_0\,. \tag{4.11}$$

It must be observed that in this case also the external massless legs acquire a non vanishing two-loop wave function renormalization factor indicated by $\delta Z_{\mathrm{WF},m}^{(2,N_h)}$. The quantity $\mathcal{A}^{(d_2,\texttt{mass CT})}$ indicates the second diagram in Fig. 4 with a mass counter term insertion in one of the internal heavy quark lines. The renormalization constant appearing for the first time in Eq. (4.11) are:

$$\begin{aligned}
\delta Z_{\alpha}^{(1,N_h)} &= C(\varepsilon)\,\frac{e^{-\gamma\varepsilon}}{\Gamma(1+\varepsilon)}\,\frac{N_h}{6\varepsilon}\,,\\
\delta Z_{m}^{(1)} &= \delta Z_{\mathrm{WF},M}^{(1)}\,,\\
\delta Z_{\alpha}^{(2,N_h)} &= C(\varepsilon)^2\left(\frac{e^{-\gamma\varepsilon}}{\Gamma(1+\varepsilon)}\right)^2\frac{1}{4\varepsilon}\left(\frac{5}{12}C_A N_h+\frac{1}{4}C_F N_h-\frac{11}{9\varepsilon}C_A N_h\right)\,,\\
\delta Z_{\mathrm{WF},M}^{(2,N_h)} &= C(\varepsilon)^2\left(\frac{\mu^2}{m^2}\right)^{2\varepsilon}C_F N_h\left(\frac{1}{8\varepsilon^2}+\frac{19}{96\varepsilon}+\frac{1139}{576}-\frac{\pi^2}{6}+\mathcal{O}(\varepsilon)\right)\,,\\
\delta Z_{\mathrm{WF},m}^{(2,N_h)} &= C(\varepsilon)^2\left(\frac{\mu^2}{m^2}\right)^{2\varepsilon}C_F N_h\left(\frac{1}{32\varepsilon}-\frac{5}{192}+\mathcal{O}(\varepsilon)\right)\,.
\end{aligned} \tag{4.12}$$

The renormalization coefficients in Eqs. (4.10,4.12) can be found in [20, 46].

The renormalization of the functions F_i $(i = l, h, lh)$ in Eq. (2.5) is trivial since the relevant two-loop diagrams are reducible and involve the insertion of two one-loop fermionic vacuum polarization insertions on the gluon propagator in the diagram of Fig. 1.

5. Results

The main result of the present paper is an analytic, non-approximated expression for the coefficients $E_l, E_h, D_l, D_h, F_l, F_{lh}, F_h$ in Eq. (2.5). Since such a result is too long to be explicitly printed here, we included in the arXiv submission of this work a text file with the complete result, which is written in terms of one-dimensional HPLs of maximum weight four and two-dimensional HPLs of maximum weight three. Since the coefficients in Eq. (2.5) still contain infrared poles, the result is dependent on the choice of a global, ε-dependent normalization factor. With our choice, we factor out an overall coefficient

$$C^2(\varepsilon) = \left[(4\pi)^{\varepsilon}\,\Gamma(1+\varepsilon)\right]^2\,. \tag{5.1}$$

We also provide two codes, one written in `Fortran`, the other as a `Mathematica` package, that numerically evaluate the analytic expression of the quantities listed above for arbitrary values of the mass scales involved in the calculation.

In order to cross check our results, we expanded them in the $s, |t|, |u| \gg m^2$ limit. The first term in the expansion agrees with the results published in [20]; the second order term agrees with the results found in the `Mathematica` files included in the arXiv version of [24]. We also find complete agreement with the numerical result of Table 3 in [24], corresponding to a phase space point in which the $s, |t|, |u| \gg m^2$ approximation cannot be applied.

It is straightforward to expand our result for values of the center of mass energy close to the production threshold. We define

$$\beta = \sqrt{1 - \frac{4m^2}{s}}\,, \qquad \xi = \frac{1-\cos\theta}{2}\,, \qquad L_\mu = \ln\left(\frac{\mu^2}{m^2}\right)\,, \qquad \ln_2 = \ln(2)\,, \tag{5.2}$$

where θ is the scattering angle in the partonic center of mass frame, and we expand our results in powers of the heavy quark velocity β, up to terms of order β^2. We find

$$\begin{aligned}
D_l(\beta,\xi) = {} & \left(-\frac{1}{4} + \mathcal{O}\left(\beta^2\right)\right)\frac{1}{\varepsilon^3} + \left[\frac{19}{36} - \frac{\ln_2}{3} + \frac{L_\mu}{6} + \left(-\frac{1}{3} + \frac{2\xi}{3}\right)\beta + \mathcal{O}\left(\beta^2\right)\right]\frac{1}{\varepsilon^2} \\
& + \left\{2\ln_2^2 - \frac{37\ln_2}{9} - \frac{2\zeta(2)}{3} + \frac{589}{216} + \left(\frac{37}{18} - 2\ln_2\right)L_\mu + \frac{L_\mu^2}{2}\right. \\
& \left. + \left[2 - \frac{4\ln_2}{3} + \left(\frac{8\ln_2}{3} - 4\right)\xi + \left(\frac{2}{3} - \frac{4\xi}{3}\right)L_\mu\right]\beta + \mathcal{O}\left(\beta^2\right)\right\}\frac{1}{\varepsilon} \\
& + \left\{-\frac{32\ln_2^3}{9} + \frac{16\ln_2^2}{9} + \frac{14\zeta(2)\ln_2}{3} + \frac{475\ln_2}{54} - \frac{13\zeta(2)}{18} - \frac{79\zeta(3)}{18} - \frac{1211}{144}\right. \\
& + \left(\frac{16\ln_2^2}{3} - \frac{4\ln_2}{3} - \frac{7\zeta(2)}{3} - \frac{163}{36}\right)L_\mu + \left(\frac{1}{9} - \frac{8\ln_2}{3}\right)L_\mu^2 + \frac{4L_\mu^3}{9} \\
& + \left[\frac{20\ln_2^2}{9} - \frac{64\ln_2}{27} - \frac{26\zeta(2)}{9} + \frac{7}{27} + \left(-\frac{40\ln_2^2}{9} + \frac{128\ln_2}{27} + \frac{52\zeta(2)}{9} - \frac{14}{27}\right)\xi\right. \\
& \left.\left. + \left(\frac{20}{9} - \frac{20\ln_2}{9} + \left(\frac{40\ln_2}{9} - \frac{40}{9}\right)\xi\right)L_\mu + \left(\frac{4}{3} - \frac{8\xi}{3}\right)L_\mu^2\right]\beta + \mathcal{O}\left(\beta^2\right)\right\} + \mathcal{O}\left(\varepsilon\right)\,, \qquad (5.3) \\
D_h(\beta,\xi) = {} & \left(\frac{8}{9} + \frac{2L_\mu}{3} + \mathcal{O}\left(\beta^2\right)\right)\frac{1}{\varepsilon^2} + \left\{-\frac{16\ln_2}{9} + \frac{\zeta(2)}{3} + \frac{88}{27} + \left(\frac{25}{9} - \frac{4\ln_2}{3}\right)L_\mu + L_\mu^2\right. \\
& \left. + \left[\frac{16}{9} - 3\zeta(2) - \frac{32\xi}{9} + \left(\frac{4}{3} - \frac{8\xi}{3}\right)L_\mu\right]\beta + \mathcal{O}\left(\beta^2\right)\right\}\frac{1}{\varepsilon} + \left\{\frac{16\ln_2^2}{9} + \frac{55\zeta(2)\ln_2}{3}\right. \\
& - \frac{148\ln_2}{27} - \frac{857\zeta(2)}{72} + \frac{283\zeta(3)}{144} - \frac{209}{108} + \left(\frac{4\ln_2^2}{3} - \frac{14\ln_2}{9} - \frac{\zeta(2)}{3} - \frac{319}{54}\right)L_\mu \\
& + \left(\frac{5}{6} - 2\ln_2\right)L_\mu^2 + \frac{7L_\mu^3}{9} + \left[12\zeta(2)\ln_2 + \frac{8\ln_2}{9} - \frac{131\zeta(2)}{18} + 6\zeta(2)\ln(\beta)\right. \\
& + \frac{214}{27} + \left(-\frac{16\ln_2}{9} - \frac{58\zeta(2)}{9} - \frac{428}{27}\right)\xi + \left(\frac{4\ln_2}{9} - 6\zeta(2) + \frac{16}{9}\right. \\
& \left.\left.\left. + \left(-\frac{8\ln_2}{9} - \frac{32}{9}\right)\xi\right)L_\mu + (2-4\xi)L_\mu^2\right]\beta + \mathcal{O}\left(\beta^2\right)\right\} + \mathcal{O}\left(\varepsilon\right)\,, \qquad (5.4) \\
E_l(\beta,\xi) = {} & \left(\frac{1}{4} + \mathcal{O}\left(\beta^2\right)\right)\frac{1}{\varepsilon^3} + \left[\frac{\ln_2}{3} - \frac{25}{36} - \frac{L_\mu}{6} + \left(\frac{4}{3} - \frac{8\xi}{3}\right)\beta + \mathcal{O}\left(\beta^2\right)\right]\frac{1}{\varepsilon^2} \\
& + \left\{\frac{\zeta(2)}{\beta} - 2\ln_2^2 + \frac{31\ln_2}{9} + \frac{8\zeta(2)}{3} - \frac{373}{216} + \left(2\ln_2 - \frac{31}{18}\right)L_\mu - \frac{L_\mu^2}{2}\right.
\end{aligned}$$

$$
\begin{aligned}
&+\left[\frac{16\ln_2}{3}+\zeta(2)-8+\left(-\frac{32\ln_2}{3}-2\zeta(2)+16\right)\xi+2\zeta(2)\xi^2\right.\\
&\left.+\left(-\frac{8}{3}+\frac{16\xi}{3}\right)L_\mu\right]\beta+\mathcal{O}\left(\beta^2\right)\Bigg\}\frac{1}{\varepsilon}+\Bigg\{\Bigg(-8\ln_2\zeta(2)-4\ln(\beta)\zeta(2)+4\zeta(2)\\
&+4\zeta(2)L_\mu\Bigg)\frac{1}{\beta}+\frac{32\ln_2^3}{9}-\frac{68\ln_2^2}{9}-\frac{50\zeta(2)\ln_2}{3}+\frac{643\ln_2}{54}+\frac{221\zeta(2)}{18}-\frac{10\zeta(3)}{9}\\
&-\frac{10285}{1296}+\left(-\frac{16\ln_2^2}{3}+\frac{68\ln_2}{9}+\frac{25\zeta(2)}{3}-\frac{787}{108}\right)L_\mu+\left(\frac{8\ln_2}{3}-\frac{17}{9}\right)L_\mu^2-\frac{4L_\mu^3}{9}\\
&+\left[-\frac{80\ln_2^2}{9}-8\zeta(2)\ln_2+\frac{256\ln_2}{27}+\frac{158\zeta(2)}{9}-4\zeta(2)\ln(\beta)-\frac{28}{27}\right.\\
&+\left(\frac{160\ln_2^2}{9}+16\zeta(2)\ln_2-\frac{512\ln_2}{27}-\frac{334\zeta(2)}{9}+8\zeta(2)\ln(\beta)+\frac{56}{27}\right)\xi\\
&+\Big(-16\ln_2\zeta(2)-8\ln(\beta)\zeta(2)+14\zeta(2)\Big)\xi^2+\left(\frac{80\ln_2}{9}+4\zeta(2)-\frac{80}{9}+\Big(-\frac{160\ln_2}{9}\right.\\
&\left.\left.-8\zeta(2)+\frac{160}{9}\Big)\xi+8\zeta(2)\xi^2\right)L_\mu+\left(-\frac{16}{3}+\frac{32\xi}{3}\right)L_\mu^2\Bigg]\beta+\mathcal{O}\left(\beta^2\right)\Bigg\}+\mathcal{O}\left(\varepsilon\right)\,, \qquad (5.5)\\
E_h(\beta,\xi)=&\left(-\frac{8}{9}-\frac{2L_\mu}{3}+\mathcal{O}\left(\beta^2\right)\right)\frac{1}{\varepsilon^2}+\Bigg\{\frac{16\ln_2}{9}+\frac{7\zeta(2)}{6}-\frac{64}{27}+\left(\frac{4\ln_2}{3}-\frac{19}{9}\right)L_\mu-L_\mu^2\\
&+\left[6\zeta(2)-\frac{64}{9}+\frac{128\xi}{9}+\left(-\frac{16}{3}+\frac{32\xi}{3}\right)L_\mu\right]\beta+\mathcal{O}\left(\beta^2\right)\Bigg\}\frac{1}{\varepsilon}\\
&+\Bigg\{\left(\frac{8\zeta(2)}{3}+2\zeta(2)L_\mu\right)\frac{1}{\beta}-\frac{16\ln_2^2}{9}-\frac{43\zeta(2)\ln_2}{3}+\frac{343\ln_2}{27}+\frac{61\zeta(2)}{9\sqrt{2}}\\
&+\frac{841\zeta(2)}{72}-\frac{83\zeta(3)}{18}-12\zeta(2)\ln(\beta)-\frac{5}{12}\mathrm{Li}_3\left(3-2\sqrt{2}\right)-\frac{61\mathrm{Li}_2\left(3-2\sqrt{2}\right)}{9\sqrt{2}}\\
&+\frac{5}{18}\ln^3\left(1+\sqrt{2}\right)-\frac{61\ln^2\left(1+\sqrt{2}\right)}{9\sqrt{2}}-\frac{5}{6}\zeta(2)\ln\left(1+\sqrt{2}\right)-\frac{6703}{324}\\
&+\left(-\frac{4\ln_2^2}{3}+\frac{38\ln_2}{9}+\frac{16\zeta(2)}{3}-\frac{463}{54}\right)L_\mu+\left(2\ln_2-\frac{41}{18}\right)L_\mu^2-\frac{7L_\mu^3}{9}\\
&+\Bigg[-24\zeta(2)\ln_2-\frac{32\ln_2}{9}+\frac{7\zeta(2)}{9}-12\zeta(2)\ln(\beta)-\frac{856}{27}+\left(\frac{64\ln_2}{9}+\frac{184\zeta(2)}{9}\right.\\
&\left.+\frac{1712}{27}\right)\xi+\frac{16\zeta(2)\xi^2}{3}+\left(-\frac{16\ln_2}{9}+14\zeta(2)-\frac{64}{9}+\left(\frac{32\ln_2}{9}-4\zeta(2)+\frac{128}{9}\right)\xi\right.\\
&\left.+4\zeta(2)\xi^2\right)L_\mu+\left(-8+16\xi\right)L_\mu^2\Bigg]\beta+\mathcal{O}\left(\beta^2\right)\Bigg\}+\mathcal{O}\left(\varepsilon\right)\,, \qquad (5.6)\\
F_l(\beta,\xi)=&\frac{2}{81}\left[(5-6\ln_2)^2-54\zeta(2)\right]+\mathcal{O}\left(\beta^2\right)+\mathcal{O}\left(\varepsilon\right)\,, \qquad (5.7)
\end{aligned}
$$

$$F_h(\beta,\xi) = \frac{128}{81} + \mathcal{O}\left(\beta^2\right) + \mathcal{O}\left(\varepsilon\right) , \tag{5.8}$$

$$F_{lh}(\beta,\xi) = \left(\frac{160}{81} - \frac{64\ln_2}{27}\right) - 4\zeta(2)\beta + \mathcal{O}\left(\beta^2\right) + \mathcal{O}\left(\varepsilon\right) . \tag{5.9}$$

These expansions could be used in the future in the calculation of logarithmically enhanced terms at production threshold.

6. Conclusions and Outlook

In this paper, we presented the analytic calculation of the two-loop fermionic corrections to the heavy-quark production amplitude for $q\bar{q} \to t\bar{t}$, retaining the exact heavy-quark mass dependence. Our work serves as an independent confirmation of recent results obtained analytically as small-mass expansions [20] and numerically [24]. We also provide new results on the threshold expansion of the amplitude.

Our result represents a gauge invariant sub-set of the full two-loop virtual correction to the partonic process $q\overline{q} \to t\overline{t}$. In order to complete the analytic calculation of the two-loop virtual corrections, it is necessary to calculate the diagrams that do not contain fermion loops, which is currently in progress. Likewise, analytic results for the two-loop amplitude for $gg \to t\bar{t}$ could be obtained in the same calculational framework.

In order to obtain NNLO predictions for the total $t\bar{t}$ production cross section and for differential distributions, it is necessary to combine the two-loop virtual corrections with the already available [10] one-loop corrections to the $t\bar{t}$+(1 parton) process and the tree-level $t\bar{t}$+(2 partons) process. Since these contribute to infrared-divergent configurations where up to two partons can become unresolved, their implementation requires the application of a NNLO subtraction method. The methods presently available [47–49] have been applied up to now [50–52] to at most $1 \to 3$ processes in e^+e^- annihilation and $2 \to 1$ processes at hadron colliders, such that a calculation of a hadronic $2 \to 2$ process, involving massive partons, will be a new step in complexity, potentially requiring further refinements of these methods.

Acknowledgments

R. B. would like to thank S. Catani for useful discussions. We are grateful to J. Vermaseren for his kind assistance in the use of `FORM` [27]. This work was supported by the Swiss National Science Foundation (SNF) under contracts 200020-117602 and PBZH2-117028. The work of D. M. was partly supported by the US Department of Energy under contract DE-AC02-76SF00515.

A. Harmonic Polylogarithms

The results of this work are conveniently expressed, in the non-physical region $s < 0$, in terms of one- and two-dimensional HPLs. Nowadays, harmonic polylogarithms are extensively used in multiloop computations, therefore in this section we just summarize

their definition; the reader interested in the algebraic properties of these functions can find detailed discussions of the topic in the available literature [44, 45].

In the process under study, five different weight functions are needed; they are

$$f_w(x) = \frac{1}{x-w}, \quad \text{with} \quad w \in \left\{0, 1, -1, -y, -\frac{1}{y}\right\}. \tag{A.1}$$

The weight-one HPLs are defined as

$$G(0;x) = \ln x, \qquad G(w;x) = \int_0^x dt f_w(t). \tag{A.2}$$

HPLs of higher weight are defined by iterated integrations

$$G(w,\cdots;x) = \int_0^x dt f_w(t) G(\cdots;t), \tag{A.3}$$

with the only exception of the HPLs in which all the weights are zero which are defined as follows

$$G(\underbrace{0,0,\cdots,0}_{n};x) = \frac{1}{n!}\ln^n x. \tag{A.4}$$

The reader should be aware of the fact that in the original definition of Remiddi and Vermaseren, the weight function corresponding to the weight 1 was $f_1 = 1/(1-x)$. In order to translate the HPLs defined with the Remiddi-Vermaseren convention to the ones employed in this work (and vice versa) it is sufficient to multiply each HPL by a factor $(-1)^n$, where n is the number of weights equal to 1.

The weights $-y$ and $-1/y$ were already introduced in [28, 45]. In our results, the two-dimensional harmonic polylogarithms have maximum weight three. As it is well known, if the weight is not larger than three, these functions can be rewritten in terms of Nielsen polylogarithms. For completeness, we list below the explicit expression of the two-dimensional harmonic polylogarithms which appear in our analytic results in terms of Nielsen's polylogarithms:

$$\begin{aligned}
G(-y;x) &= \ln\left(\frac{x+y}{y}\right), \\
G(-1/y;x) &= \ln(1+xy), \\
G(-y,0;x) &= \ln(x)\ln\left(\frac{x+y}{y}\right) + \mathrm{Li}_2\left(-\frac{x}{y}\right), \\
G(-1/y,0;x) &= \ln(x)\ln(xy+1) + \mathrm{Li}_2(-xy), \\
G(-y,1;x) &= \frac{1}{2}\ln^2(y+1) - \ln(1-x)\ln(y+1) - \ln(y)\ln(y+1) \\
&\quad + \ln(1-x)\ln(x+y) - \mathrm{Li}_2(-y) + \mathrm{Li}_2\left(\frac{1-x}{y+1}\right) - \frac{\pi^2}{6}, \\
G(-1/y,1;x) &= \frac{1}{2}\ln^2(y+1) - \ln(1-x)\ln(y+1) + \ln(1-x)\ln(xy+1) \\
&\quad + \mathrm{Li}_2(-y) + \mathrm{Li}_2\left(\frac{y-xy}{y+1}\right),
\end{aligned}$$

$$
\begin{aligned}
G(-y,0,0;x) &= \frac{1}{2}\ln^2(x)\ln\left(1+\frac{x}{y}\right)+\ln(x)\mathrm{Li}_2\left(-\frac{x}{y}\right)-\mathrm{Li}_3\left(-\frac{x}{y}\right)\,,\\
G(-1/y,0,0;x) &= \frac{1}{2}\ln^2(x)\ln\left(1+xy\right)+\ln(x)\mathrm{Li}_2\left(-xy\right)-\mathrm{Li}_3\left(-xy\right)\,,\\
G(-y,1,0;x) &= -\frac{1}{3}\ln^3(1-x)-\ln(x)\ln^2(1-x)-\ln(y)\ln^2(1-x)+\frac{1}{2}\ln(y+1)\ln^2(1-x)\\
&\quad+\ln(x+y)\ln^2(1-x)-\frac{1}{2}\ln^2(y+1)\ln(1-x)-\ln^2(x+y)\ln(1-x)\\
&\quad-\ln(x)\ln(y)\ln(1-x)-\ln(x)\ln(y+1)\ln(1-x)+\ln(y)\ln(y+1)\ln(1-x)\\
&\quad+2\ln(x)\ln(x+y)\ln(1-x)+\ln(y)\ln(x+y)\ln(1-x)\\
&\quad-\mathrm{Li}_2(x)\ln(1-x)+\mathrm{Li}_2\left(-\frac{x}{y}\right)\ln(1-x)+\mathrm{Li}_2(-y)\ln(1-x)\\
&\quad-\mathrm{Li}_2\left(\frac{(1-x)y}{x+y}\right)\ln(1-x)-\mathrm{Li}_2\left(\frac{x+y}{x-1}\right)\ln(1-x)-\frac{1}{3}\pi^2\ln(1-x)\\
&\quad+\frac{1}{2}\ln(x)\ln^2(y+1)-\frac{1}{6}\pi^2\ln(x)-\ln(x)\ln(y)\ln(y+1)-\ln(y)\mathrm{Li}_2(x)\\
&\quad+\ln(x+y)\mathrm{Li}_2(x)-\ln(x)\mathrm{Li}_2(-y)+\ln(x)\mathrm{Li}_2\left(\frac{1-x}{y+1}\right)+\ln(y)\mathrm{Li}_2\left(\frac{y}{x+y}\right)\\
&\quad-\ln(x+y)\mathrm{Li}_2\left(\frac{y}{x+y}\right)+\ln(y)\mathrm{Li}_2\left(\frac{(1-x)y}{x+y}\right)+\ln(x+y)\mathrm{Li}_2\left(\frac{(1-x)y}{x+y}\right)\\
&\quad-\ln(y)\mathrm{Li}_2\left(\frac{x+y}{x-1}\right)+\ln(x+y)\mathrm{Li}_2\left(\frac{x+y}{x-1}\right)-\mathrm{Li}_3(1-x)-\mathrm{Li}_3\left(\frac{x}{x-1}\right)\\
&\quad-\mathrm{Li}_3\left(-\frac{x}{y}\right)-\mathrm{Li}_3(-y)+\mathrm{Li}_3\left(\frac{1}{y+1}\right)-\mathrm{Li}_3\left(\frac{1-x}{y+1}\right)\\
&\quad+\mathrm{Li}_3\left(\frac{x(y+1)}{(x-1)y}\right)-\mathrm{Li}_3\left(\frac{y}{x+y}\right)+\mathrm{Li}_3\left(\frac{(1-x)y}{x+y}\right)-\mathrm{Li}_3\left(\frac{x+y}{x-1}\right)+\zeta(3)\,,\\
G(-1/y,1,0;x) &= -\frac{1}{3}\ln^3(1-x)-\ln(x)\ln^2(1-x)-\frac{1}{2}\ln(y)\ln^2(1-x)\\
&\quad+\frac{1}{2}\ln(y+1)\ln^2(1-x)+\ln(xy+1)\ln^2(1-x)-\frac{1}{2}\ln^2(y+1)\ln(1-x)\\
&\quad-\ln^2(xy+1)\ln(1-x)-\ln(x)\ln(y+1)\ln(1-x)\\
&\quad+2\ln(x)\ln(xy+1)\ln(1-x)+\ln(y)\ln(xy+1)\ln(1-x)-\mathrm{Li}_2(x)\ln(1-x)\\
&\quad-\mathrm{Li}_2(-y)\ln(1-x)+\mathrm{Li}_2(-xy)\ln(1-x)-\mathrm{Li}_2\left(\frac{1-x}{xy+1}\right)\ln(1-x)\\
&\quad-\mathrm{Li}_2\left(\frac{xy+1}{(x-1)y}\right)\ln(1-x)+\frac{1}{6}\pi^2\ln(1-x)+\frac{1}{2}\ln(x)\ln^2(y+1)\\
&\quad+\ln(xy+1)\mathrm{Li}_2(x)+\ln(x)\mathrm{Li}_2(-y)+\ln(x)\mathrm{Li}_2\left(\frac{y-xy}{y+1}\right)\\
&\quad-\ln(xy+1)\mathrm{Li}_2\left(\frac{1}{xy+1}\right)+\ln(xy+1)\mathrm{Li}_2\left(\frac{1-x}{xy+1}\right)\\
&\quad+\ln(xy+1)\mathrm{Li}_2\left(\frac{xy+1}{(x-1)y}\right)-\mathrm{Li}_3\left(1-x\right)-\mathrm{Li}_3\left(\frac{x}{x-1}\right)+\mathrm{Li}_3\left(-\frac{1}{y}\right)\\
&\quad-\mathrm{Li}_3(-xy)+\mathrm{Li}_3\left(\frac{y}{y+1}\right)+\mathrm{Li}_3\left(\frac{x(y+1)}{x-1}\right)-\mathrm{Li}_3\left(\frac{y-xy}{y+1}\right)
\end{aligned}
$$

$$
\begin{aligned}
&-\mathrm{Li}_3\left(\frac{1}{xy+1}\right)+\mathrm{Li}_3\left(\frac{1-x}{xy+1}\right)-\mathrm{Li}_3\left(\frac{xy+1}{(x-1)y}\right)+\zeta(3)\,,\\
G(-y,0,1;x) &= \frac{1}{3}\ln^3(1-x)+\ln(x)\ln^2(1-x)+\frac{1}{2}\ln(y)\ln^2(1-x)-\ln(x+y)\ln^2(1-x)\\
&+\ln^2(x+y)\ln(1-x)+\ln(x)\ln(y)\ln(1-x)-\ln(x)\ln(x+y)\ln(1-x)\\
&-\ln(y)\ln(x+y)\ln(1-x)+\mathrm{Li}_2(x)\ln(1-x)+\mathrm{Li}_2\left(\frac{(1-x)y}{x+y}\right)\ln(1-x)\\
&+\mathrm{Li}_2\left(\frac{x+y}{x-1}\right)\ln(1-x)-\frac{1}{6}\pi^2\ln(1-x)+\ln(y)\mathrm{Li}_2(x)\\
&-\ln(x+y)\mathrm{Li}_2(x)-\ln(y)\mathrm{Li}_2\left(\frac{y}{x+y}\right)+\ln(x+y)\mathrm{Li}_2\left(\frac{y}{x+y}\right)\\
&+\ln(y)\mathrm{Li}_2\left(\frac{(1-x)y}{x+y}\right)-\ln(x+y)\mathrm{Li}_2\left(\frac{(1-x)y}{x+y}\right)+\ln(y)\mathrm{Li}_2\left(\frac{x+y}{x-1}\right)\\
&-\ln(x+y)\mathrm{Li}_2\left(\frac{x+y}{x-1}\right)+\mathrm{Li}_3(1-x)-\mathrm{Li}_3(-y)+\mathrm{Li}_3\left(\frac{y}{x+y}\right)\\
&-\mathrm{Li}_3\left(\frac{(1-x)y}{x+y}\right)+\mathrm{Li}_3\left(\frac{x+y}{x-1}\right)-\zeta(3)\,,\\
G(-1/y,0,1;x) &= \frac{1}{3}\ln^3(1-x)+\ln(x)\ln^2(1-x)+\frac{1}{2}\ln(y)\ln^2(1-x)\\
&-\ln(xy+1)\ln^2(1-x)+\ln^2(xy+1)\ln(1-x)-\ln(x)\ln(xy+1)\times\\
&\times\ln(1-x)-\ln(y)\ln(xy+1)\ln(1-x)+\mathrm{Li}_2\left(\frac{1-x}{xy+1}\right)\ln(1-x)\\
&+\mathrm{Li}_2\left(\frac{xy+1}{(x-1)y}\right)\ln(1-x)-\frac{1}{6}\pi^2\ln(1-x)+\ln\left(\frac{1-x}{xy+1}\right)\mathrm{Li}_2(x)\\
&+\ln(xy+1)\mathrm{Li}_2\left(\frac{1}{xy+1}\right)-\ln(xy+1)\mathrm{Li}_2\left(\frac{1-x}{xy+1}\right)\\
&-\ln(xy+1)\mathrm{Li}_2\left(\frac{xy+1}{(x-1)y}\right)+\mathrm{Li}_3(1-x)-\mathrm{Li}_3\left(-\frac{1}{y}\right)\\
&+\mathrm{Li}_3\left(\frac{1}{xy+1}\right)-\mathrm{Li}_3\left(\frac{1-x}{xy+1}\right)+\mathrm{Li}_3\left(\frac{xy+1}{(x-1)y}\right)-\zeta(3)\,,\\
G(-y,1,1;x) &= -\frac{1}{2}\ln(y+1)\ln^2(1-x)+\frac{1}{2}\ln(x+y)\ln^2(1-x)\\
&+\mathrm{Li}_2\left(\frac{1-x}{y+1}\right)\ln(1-x)+\mathrm{Li}_3\left(\frac{1}{y+1}\right)-\mathrm{Li}_3\left(\frac{1-x}{y+1}\right)\,,\\
G(-1/y,1,1;x) &= -\frac{1}{2}\ln(y+1)\ln^2(1-x)+\frac{1}{2}\ln(xy+1)\ln^2(1-x)\\
&+\mathrm{Li}_2\left(\frac{y-xy}{y+1}\right)\ln(1-x)+\mathrm{Li}_3\left(\frac{y}{y+1}\right)-\mathrm{Li}_3\left(\frac{y-xy}{y+1}\right)\,. \qquad \text{(A.5)}
\end{aligned}
$$

We first obtained the squared matrix elements in the non-physical region $s < 0$. The corresponding quantities in the physical region $s > 0$ could be obtained by analytic continuation to the complex value $s \to s + i\delta$, where $\delta \to 0^+$. For $s > 4m^2$ the variable x becomes

$$x = -x' + i\delta\,, \qquad \text{(A.6)}$$

where

$$x' = \frac{\sqrt{s} - \sqrt{s-4m^2}}{\sqrt{s} + \sqrt{s-4m^2}}\,, \tag{A.7}$$

So that $0 < x' < 1$ for $4m^2 < s < \infty$. While the HPLs with argument y and z are always real, the HPLs of x are complex for $s > 0$. In particular, the imaginary part of the HPLs of argument x for $s > 4m^2$ is defined when the analytic continuation of the logarithm is specified:

$$G(0;x) \to G(0;-x'+i\delta) = G(0,x') + i\pi\,. \tag{A.8}$$

In the quantities E_h and D_h one also encounters the variable x_p defined in Eq. (3.2). In this case, in the physical region one finds that

$$x_p \to -x_p' + i\delta\,, \tag{A.9}$$

where

$$x_p' = \frac{\sqrt{s+4m^2} - \sqrt{s}}{\sqrt{s+4m^2} + \sqrt{s}}\,; \tag{A.10}$$

therefore $0 < x_p < 1$ when $0 < s < \infty$. The imaginary part of the HPLs of argument x_p' is defined according to the same principle that determines the imaginary part of the HPLs of argument x (Eq.(A.8)). The analytic continuation of the two-dimensional HPLs presented in this appendix is determined by the analytic properties of the functions ln, Li_2 and Li_3.

B. Master Integrals

In this Appendix we collect the MIs for the topologies in Fig. 2-(k), Fig. 2-(l), Fig. 3-(k), and in Fig. 3-(l) that are not yet available in the literature.

The explicit expression of the MIs depends on the chosen normalization of the integration measure. The integration on the loop momenta is normalized as follows

$$\int \mathfrak{D}^d k = \frac{1}{C(\varepsilon)} \left(\frac{\mu^2}{m^2}\right)^{-\varepsilon} \int \frac{d^d k}{(4\pi^2)^{(1-\varepsilon)}}\,, \tag{B.1}$$

where $C(\varepsilon)$ was defined in Eq. (5.1). In Eq. (B.1) μ stands for the 't Hooft mass of dimensional regularization. The integration measure in Eq. (B.1) is chosen in such a way that the one-loop massive tadpole becomes

$$\int \mathfrak{D}^d k \; \frac{1}{k^2+m^2} = -\frac{m^2}{4(1-\varepsilon)\varepsilon}\,. \tag{B.2}$$

In calculating the squared matrix element, we multiply our bare results by $(\mu^2/m^2)^\varepsilon$, in order to make explicit the dependence on the top scale. We also point out that, since the squared matrix element still contains soft and collinear divergencies regulated by ε, it depends on the normalization of the integration measure. In particular, in order to match our results with the ones of [20, 24], it is necessary to multiply them by the factor

$$\frac{e^{-2\gamma\varepsilon}}{\Gamma\left(1+\varepsilon\right)^2} = 1 - \zeta(2)\varepsilon^2 + \frac{2}{3}\zeta(3)\varepsilon^3 + \mathcal{O}\left(\varepsilon^4\right)\,. \tag{B.3}$$

There is a single MIs belonging to the topology Fig. 2-(k) :

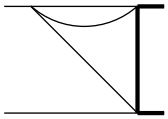

$$= \int \frac{\mathfrak{D}^d k_1 \mathfrak{D}^d k_2}{P_0\left(k_1+p_1\right) P_0\left(k_2\right) P_0\left(k_1-k_2\right) P_m\left(k_1+p_3\right)}\,, \tag{B.4}$$

where we define

$$P_0\left(k\right) \equiv k^2\,, \qquad P_m\left(k\right) \equiv k^2+m^2\,; \tag{B.5}$$

we then find

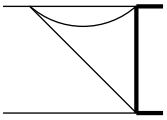

$$= \sum_{i=-2}^{1} A_i\, \varepsilon^i + \mathcal{O}(\varepsilon^2)\,, \tag{B.6}$$

$$\begin{aligned}
A_{-2} &= \frac{1}{32}\,,\\
A_{-1} &= \frac{1}{32y}\left[5y - 2\left(1+y\right) G\left(-1;y\right)\right]\,,\\
A_0 &= \frac{1}{32y}\left[19y + 4y\zeta(2) - 10\left(1+y\right) G\left(-1;y\right)\right.\\
&\quad \left. +8\left(1+y\right) G\left(-1,-1;y\right) - 4G\left(0,-1;y\right) - 4yG\left(0,-1;y\right)\right]\,,\\
A_1 &= \frac{1}{32y}\Big[65y + 20y\zeta\left(2\right) + 8y\zeta\left(3\right) - 2\left(1+y\right)\left(19+4\zeta\left(2\right)\right) G\left(-1;y\right)\\
&\quad +40\left(1+y\right) G\left(-1,-1;y\right) - 20G\left(0,-1,y\right) - 20yG\left(0,-1;y\right) - 32G\left(-1,-1,-1;y\right)\\
&\quad -32yG\left(-1,-1,-1;y\right) + 16G\left(-1,0,-1,y\right) + 16yG\left(-1,0,-1;y\right)\\
&\quad +16G\left(0,-1,-1;y\right) + 16yG\left(0,-1,-1;y\right) - 8G\left(0,0,-1;y\right) - \text{`}8yG\left(0,0,-1;y\right)\Big]\,.
\end{aligned} \tag{B.7}$$

Also the four point topology Fig. 2-(l) has a single MI:

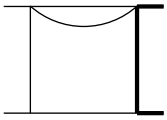

$$= \int \frac{\mathfrak{D}^d k_1 \mathfrak{D}^d k_2}{P_0\left(k_1+p_1\right) P_0\left(k_1+p_1+p_2\right) P_0\left(k_2\right) P_0\left(k_1-k_2\right) P_m\left(k_1+p_3\right)}\,, \tag{B.8}$$

with

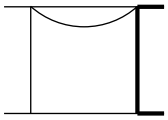

$$= \frac{1}{m^2} \sum_{i=-3}^{0} A_i\, \varepsilon + \mathcal{O}(\varepsilon)\,, \tag{B.9}$$

$$\begin{aligned}
A_{-3} &= \frac{1}{32(y+1)}\,,\\
A_{-2} &= \frac{1}{32(y+1)}\left(G(0;x) - 2G(1;x) - 2G(-1;y) + 2\right)\,,
\end{aligned}$$

$$
\begin{aligned}
A_{-1} = \frac{1}{32(y+1)} \Big[& -3\zeta(2) + G(0,0;x) - 2G(0,1;x) - 2G(1,0;x) + 4G(1,1;x) \\
& + G(0;x)(2 - 2G(-1;y)) - 4G(-1;y) + G(1;x)(4G(-1;y) - 4) \\
& + 4G(-1,-1;y) - 2G(0,-1;y) + 4 \Big] ,
\end{aligned}
$$

$$
\begin{aligned}
A_0 = \frac{1}{32(y+1)} \Big[& -2(3\zeta(2) + 4\zeta(3) - 4) + G(0,0,0;x) - 2G(0,0,1;x) - 2G(0,1,0;x) \\
& + 4G(0,1,1;x) - 2G\left(-1/y,0,0,x\right) + 4G\left(-1/y,0,1,x\right) + 2G\left(-1/y,1,0,x\right) \\
& - 4G\left(-1/y,1,1,x\right) + 2G(-y,1,0;x) - 4G(-y,1,1;x) + G(1,1;x)(8 - 16G(-1;y)) \\
& + G(0,0;x)(2 - 2G(-1;y)) + 2(3\zeta(2) - 4)G(-1;y) - 2G\left(-1/y,0,x\right) G(-1;y) \\
& + 4G\left(-1/y,1,x\right) G(-1;y) - 2G(-y,0;x)G(-1;y) + 4G(-y,1;x)G(-1;y) \\
& + G(0,1;x)(4G(-1;y) - 4) + G(1,0;x)(8G(-1;y) - 4) \\
& + G(1;x)(2(7\zeta(2) - 4) + 8G(-1;y)) + 8G(-1,-1;y) \\
& + G(0;x)(-3\zeta(2) - 4G(-1;y) + 4G(-1,-1;y) - 2G(0,-1;y) + 4) \\
& - 4G(0,-1;y) + G(-y;x)(2G(0,-1;y) - 4G(-1,-1;y)) \\
& + G\left(-1/y,x\right)(-8\zeta(2) - 4G(-1,-1;y) + 2G(0,-1;y)) \\
& - 8G(-1,-1,-1;y) + 4G(-1,0,-1;y) + 4G(0,-1,-1;y) - 2G(0,0,-1;y) \Big] . \qquad \text{(B.10)}
\end{aligned}
$$

We now consider the MIs involved in the calculation of the part of the amplitude proportional to N_h. Topology Fig. 3-(k) has two MIs:

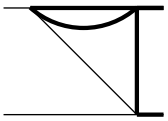

$$
= \int \frac{\mathfrak{D}^d k_1 \mathfrak{D}^d k_2}{P_0\left(k_1+p_1\right) P_m\left(k_2\right) P_m\left(k_1-k_2\right) P_m\left(k_1+p_3\right)} , \qquad \text{(B.11)}
$$

with

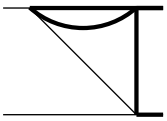

$$
= \sum_{i=-2}^{1} A_i\, \varepsilon + \mathcal{O}\left(\varepsilon\right) , \qquad \text{(B.12)}
$$

$$
A_{-2} = \frac{1}{32},
$$

$$
A_{-1} = \frac{1}{32y} \left[5y - 2(y+1)G(-1;y)\right] ,
$$

$$
\begin{aligned}
A_0 = \frac{1}{32y(y+1)} \Big[& -10G(-1;y)(y+1)^2 + 4G(-1,-1;y)(y+1)^2 - 4G(0,-1;y)(y+1) \\
& - 4yG(0,0,-1;y) + y\left(19y - 4\zeta(3) + 19\right) \Big] ,
\end{aligned}
$$

$$
\begin{aligned}
A_1 = \frac{1}{32y(y+1)} \Big[& 20G(-1,-1;y)(y+1)^2 - 8G(-1,-1,-1;y)(y+1)^2 \\
& + 8G(-1,0,-1;y)(y+1) + 8G(0,-1,-1;y)(y+1) - 8(y-1)G(1,0,-1;y)(y+1) \\
& + 4(y-1)G(1;y)\zeta(2)(y+1) + 4(y-2)(2y+1)G(0,0,-1;y) - 8yG(-1,0,0,-1;y)
\end{aligned}
$$

$$
\begin{aligned}
&+8yG(0,-1,0,-1;y)+8yG(0,0,-1,-1;y)-12yG(0,0,0,-1;y)\\
&+16yG(0,1,0,-1;y)-8yG(0,1;y)\zeta(2)+4G(0,-1;y)\left(2\zeta(2)y-5y-5\right)\\
&-2G(-1;y)\left(2\zeta(2)y^2+19y^2+4\zeta(3)y+38y-2\zeta(2)+19\right)+\frac{y}{5}\left(6\zeta(2)^2+325y\right.\\
&\left.+20y\zeta(3)-40\zeta(3)+325\right)\Big]\,. \qquad \text{(B.13)}
\end{aligned}
$$

As second MI for the topology Fig. 3-(k), we chose

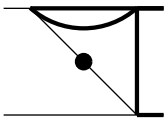

$$
= \int \frac{\mathfrak{D}^d k_1 \mathfrak{D}^d k_2}{P_0^2\left(k_1+p_1\right) P_m\left(k_2\right) P_m\left(k_1-k_2\right) P_m\left(k_1+p_3\right)}\,, \qquad \text{(B.14)}
$$

where

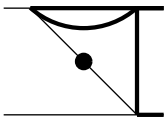

$$
= \frac{1}{m^2}\sum_{i=-2}^{1} A_i\,\varepsilon^i + \mathcal{O}\left(\varepsilon^2\right)\,, \qquad \text{(B.15)}
$$

$$
\begin{aligned}
A_{-2} &= -\frac{1}{16(y+1)},\\
A_{-1} &= \frac{y-1}{16y(y+1)}G(-1;y)\,,\\
A_0 &= \frac{y-1}{8y(y+1)^2}\Big[(y+1)G(-1;y)-(y+1)G(-1,-1;y)\\
&\quad -G(0,-1;y)+\frac{2y}{1-y}\left(y-\zeta(2)+1\right)\Big]\,,\\
A_1 &= \frac{y-1}{8y(y+1)^2}\Big[-2(y+1)G(-1,-1;y)+2G(0,-1;y)+2(y+1)G(-1,-1,-1;y)\\
&\quad -2G(-1,0,-1;y)-2G(0,-1,-1;y)-2(y-1)G(0,0,-1;y)\\
&\quad +2(y-1)G(1,0,-1;y)-(y-1)G(1;y)\zeta(2)+G(-1;y)\left(\zeta(2)y+2y-\zeta(2)+2\right)\\
&\quad -\frac{y}{y-1}\left(12\ln(2)\zeta(2)-4\zeta(2)+y\zeta(3)-8\zeta(3)\right)\Big]\,. \qquad \text{(B.16)}
\end{aligned}
$$

The box topology Fig. 3-(l), has also two MIs: the first one is

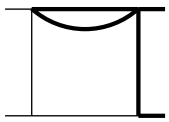

$$
= \int \frac{\mathfrak{D}^d k_1 \mathfrak{D}^d k_2}{P_0\left(k_1+p_1\right) P_0\left(k_1+p_1+p_2\right) P_m\left(k_2\right) P_m\left(k_1-k_2\right) P_m\left(k_1+p_3\right)}\,, \qquad \text{(B.17)}
$$

with

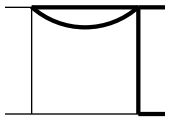

$$
= \frac{1}{m^2}\sum_{i=-3}^{0} A_i\,\varepsilon^i + \mathcal{O}\left(\varepsilon\right)\,, \qquad \text{(B.18)}
$$

$$
\begin{aligned}
A_{-3} &= \frac{1}{32(y+1)}\,,\\
A_{-2} &= \frac{1}{32(x-1)(y+1)}\,\Big[-2G(-1;y)(x-1)+2(x-1)-(1+x)G(0;x)\Big]\,,\\
A_{-1} &= \frac{1}{32(x-1)(y+1)}\Big[3\zeta(2)x+4x+6(x+1)G(-1,0;x)+(-5x-1)G(0,0;x)\\
&\quad -4(x-1)G(-1;y)+G(0;x)(2(x+1)G(-1;y)-2(x+1))+4(x-1)G(-1,-1;y)\\
&\quad -2(x-1)G(0,-1;y)+3\zeta(2)-4\Big]\,,\\
A_{0} &= \frac{1}{32(x-1)(y+1)}\Big[-36(x+1)G(-1,-1,0;x)+18(x+1)G(-1,0,0;x)\\
&\quad +6(5x+1)G(0,-1,0;x)+(-5x-1)G(0,0,0;x)-2(5x-3)G(1,0,0;x)\\
&\quad +4(x+1)G(1,1,0;x)+2(x+1)G\left(-1/y,0,0,x\right)-2(x+1)G\left(-1/y,1,0,x\right)\\
&\quad -2(x+1)G(-y,1,0;x)-4(x+1)G(1,0;x)G(-1;y)+2(x+1)G\left(-1/y,0,x\right)G(-1;y)\\
&\quad +2(x+1)G(-y,0;x)G(-1;y)+G(-1,0;x)(12(x+1)-12(x+1)G(-1;y))\\
&\quad +G(0,0;x)(2(5x+1)G(-1;y)-2(5x+1))+8(x-1)G(-1,-1;y)\\
&\quad -4(x-1)G(0,-1;y)-2(x+1)G(-y;x)G(0,-1;y)-8(x-1)G(-1,-1,-1;y)\\
&\quad +4(x-1)G(-1,0,-1;y)+4(x-1)G(0,-1,-1;y)-2(3x-1)G(0,0,-1;y)\\
&\quad -18(x+1)G(-1;x)\zeta(2)-4(x+1)G(1;x)\zeta(2)-2G(-1;y)\left(3\zeta(2)x+4x+3\zeta(2)-4\right)\\
&\quad +G(0;x)(15\zeta(2)x-4x+4(x+1)G(-1;y)-4(x+1)G(-1,-1;y)\\
&\quad +2(x+1)G(0,-1;y)+3\zeta(2)-4)+G\left(-1/y,x\right)\left(2(x+1)G(0,-1;y)+4(x+1)\zeta(2)\right)\\
&\quad +2\left(3\zeta(2)x+12\zeta(3)x+4x+3\zeta(2)+4\zeta(3)-4\right)\Big]\,. \qquad \text{(B.19)}
\end{aligned}
$$

As second MI for topology Fig. 3-(l) we chose

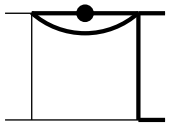

$$
= \int \frac{\mathfrak{D}^d k_1 \mathfrak{D}^d k_2}{P_0\left(k_1+p_1\right) P_0\left(k_1+p_1+p_2\right) P_m^2\left(k_2\right) P_m\left(k_1-k_2\right) P_m\left(k_1+p_3\right)}\,, \qquad \text{(B.20)}
$$

with

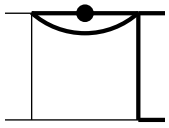

$$
= \frac{1}{m^4}\sum_{i=-2}^{0} A_i\,\varepsilon^i + \mathcal{O}\left(\varepsilon\right)\,, \qquad \text{(B.21)}
$$

$$
\begin{aligned}
A_{-2} &= \frac{x}{32(x-1)(x+1)(y+1)}\,G(0;x)\,,\\
A_{-1} &= -\frac{x}{32(x-1)(x+1)(y+1)}\Big[6G(-1,0;x)-3G(0,0;x)+2G(0;x)G(-1;y)+3\zeta(2)\Big]\,,\\
A_{0} &= -\frac{x}{32(x-1)(x+1)(y+1)}\Big[18G(-1,0,0;x)-36G(-1,-1,0;x)+18G(0,-1,0;x)
\end{aligned}
$$

$$
\begin{aligned}
&-3G(0,0,0;x)-2G(1,0,0;x)+4G(1,1,0;x)+2G\left(-1/y,0,0,x\right)-2G\left(-1/y,1,0,x\right)\\
&-2G(-y,1,0;x)-12G(-1,0;x)G(-1;y)+6G(0,0;x)G(-1;y)\\
&-4G(1,0;x)G(-1;y)+2G\left(-1/y,0,x\right)G(-1;y)+2G(-y,0;x)G(-1;y)\\
&-2G(-y;x)G(0,-1;y)-2G(0,0,-1;y)-18G(-1;x)\zeta(2)-4G(1;x)\zeta(2)\\
&-6G(-1;y)\zeta(2)+G\left(-1/y,x\right)\left(2G(0,-1;y)+4\zeta(2)\right)\\
&+G(0;x)\left(-4G(-1,-1;y)+2G(0,-1;y)+9\zeta(2)\right)+16\zeta(3)\Big]\,. \qquad \text{(B.22)}
\end{aligned}
$$

References

[1] F. Abe *et al.* [CDF Collaboration], Phys. Rev. Lett. **74** (1995) 2626 [hep-ex/9503002]; S. Abachi *et al.* [D0 Collaboration], Phys. Rev. Lett. **74**, (1995) 2632 [hep-ex/9503003].

[2] P. Nason, S. Dawson and R.K. Ellis, Nucl. Phys. B **303** (1988) 607.

[3] P. Nason, S. Dawson and R.K. Ellis, Nucl. Phys. B **327** (1989) 49 [Erratum-ibid. B **335** (1990) 260].

[4] W. Beenakker, H. Kuijf, W.L. van Neerven and J. Smith, Phys. Rev. D **40** (1989) 54.

[5] W. Beenakker, W.L. van Neerven, R. Meng, G.A. Schuler and J. Smith, Nucl. Phys. B **351** (1991) 507.

[6] M.L. Mangano, P. Nason and G. Ridolfi, Nucl. Phys. B **373** (1992) 295.

[7] J.G. Körner and Z. Merebashvili, Phys. Rev. D **66** (2002) 054023 [hep-ph/0207054].

[8] W. Bernreuther, A. Brandenburg, Z.G. Si and P. Uwer, Nucl. Phys. B **690** (2004) 81 [hep-ph/0403035].

[9] B.W. Harris, E. Laenen, L. Phaf, Z. Sullivan and S. Weinzierl, Phys. Rev. D **66** (2002) 054024 [hep-ph/0207055].

[10] S. Dittmaier, P. Uwer and S. Weinzierl, Phys. Rev. Lett. **98** (2007) 262002 [hep-ph/0703120].

[11] A. Lazopoulos, T. McElmurry, K. Melnikov and F. Petriello, arXiv:0804.2220.

[12] N. Kidonakis and G. Sterman, Nucl. Phys. B **505** (1997) 321 [hep-ph/9705234].

[13] R. Bonciani, S. Catani, M.L. Mangano and P. Nason, Nucl. Phys. B **529** (1998) 424 [hep-ph/9801375].

[14] M. Cacciari, S. Frixione, M.L. Mangano, P. Nason and G. Ridolfi, JHEP **0404** (2004) 068 [hep-ph/0303085].

[15] J.H. Kühn, A. Scharf and P. Uwer, Eur. Phys. J. C **45** (2006) 139 [hep-ph/0508092]; Eur. Phys. J. C **51** (2007) 37 [hep-ph/0610335].

[16] W. Bernreuther, M. Fücker and Z.G. Si, Phys. Rev. D **74** (2006) 113005 [hep-ph/0610334]; arXiv:0804.1237.

[17] S. Moch and P. Uwer, arXiv:0804.1476.

[18] M. Cacciari, S. Frixione, M.L. Mangano, P. Nason and G. Ridolfi, arXiv:0804.2800.

[19] N. Kidonakis and R. Vogt, arXiv:0805.3844.

[20] M. Czakon, A. Mitov and S. Moch, Phys. Lett. B **651** (2007) 147 [arXiv:0705.1975].

[21] M. Czakon, A. Mitov and S. Moch, Nucl. Phys. B **798** (2008) 210 [arXiv:0707.4139].

[22] Z. Bern, L.J. Dixon and A. Ghinculov, Phys. Rev. D **63** (2001) 053007 [hep-ph/0010075];
C. Anastasiou, E.W.N. Glover, C. Oleari and M.E. Tejeda-Yeomans, Nucl. Phys. B **601** (2001) 318 [hep-ph/0010212];
E.W.N. Glover, JHEP **0404** (2004) 021 [hep-ph/0401119].

[23] C. Anastasiou, E.W.N. Glover, C. Oleari and M.E. Tejeda-Yeomans, Nucl. Phys. B **605** (2001) 486 [hep-ph/0101304];
E.W.N. Glover and M.E. Tejeda-Yeomans, JHEP **0306** (2003) 033 [hep-ph/0304169];
Z. Bern, A. De Freitas and L.J. Dixon, JHEP **0306** (2003) 028 [hep-ph/0304168].

[24] M. Czakon, Phys. Lett. B **664** (2008) 307 [arXiv:0803.1400].

[25] J.G. Körner, Z. Merebashvili and M. Rogal, Phys. Rev. D **73** (2006) 034030 [hep-ph/0511264]; arXiv:0802.0106.

[26] P. Nogueira, J. Comput. Phys. **105** (1993) 279.

[27] J.A.M. Vermaseren, Symbolic Manipulation with `FORM`, Version 2, CAN, Amsterdam, 1991; "New features of FORM" [math-ph/0010025].

[28] R. Bonciani, A. Ferroglia, P. Mastrolia, E. Remiddi and J. J. van der Bij, Nucl. Phys. B **681** (2004) 261 [Erratum-ibid. B **702** (2004) 364] [hep-ph/0310333].

[29] R. Bonciani, A. Ferroglia and A.A. Penin, Phys. Rev. Lett. **100** (2008) 131601 [arXiv:0710.4775]; JHEP **0802** (2008) 080 [arXiv:0802.2215];
S. Actis, M. Czakon, J. Gluza and T. Riemann, Nucl. Phys. B **786** (2007) 26 [arXiv:0704.2400]; Phys. Rev. Lett. **100** (2008) 131602 [arXiv:0711.3847].

[30] S. Laporta and E. Remiddi, Phys. Lett. B **379** (1996) 283 [hep-ph/9602417].
S. Laporta, Int. J. Mod. Phys. A **15** (2000) 5087 [hep-ph/0102033].
F.V. Tkachov, Phys. Lett. B **100** (1981) 65.
K.G. Chetyrkin and F.V. Tkachov, Nucl. Phys. B **192** (1981) 159.

[31] M. Argeri, P. Mastrolia and E. Remiddi, Nucl. Phys. B **631** (2002) 388 [hep-ph/0202123].

[32] R. Bonciani, P. Mastrolia and E. Remiddi, Nucl. Phys. B **661** (2003) 289 [Erratum-ibid. B **702** (2004) 359] [hep-ph/0301170].

[33] J. Fleischer, A.V. Kotikov and O.L. Veretin, Nucl. Phys. B **547** (1999) 343 [hep-ph/9808242].
U. Aglietti and R. Bonciani, Nucl. Phys. B **668** (2003) 3 [hep-ph/0304028].

[34] A.I. Davydychev and M.Y. Kalmykov, Nucl. Phys. B **699** (2004) 3 [hep-th/0303162].

[35] R. Bonciani, P. Mastrolia and E. Remiddi, Nucl. Phys. B **690** (2004) 138 [hep-ph/0311145].

[36] U. Aglietti and R. Bonciani, Nucl. Phys. B **698** (2004) 277 [hep-ph/0401193].

[37] M. Czakon, J. Gluza and T. Riemann, Phys. Rev. D **71** (2005) 073009 [hep-ph/0412164].

[38] W. Bernreuther, *et al.*, Nucl. Phys. B **706** (2005) 245 [hep-ph/0406046]; Nucl. Phys. B **712** (2005) 229 [hep-ph/0412259]; Nucl. Phys. B **723** (2005) 91 [hep-ph/0504190]. Phys. Rev. D **72** (2005) 096002 [hep-ph/0508254]. Phys. Rev. Lett. **95** (2005) 261802 [hep-ph/0509341].

[39] R. Bonciani and A. Ferroglia, Phys. Rev. D **72** (2005) 056004 [hep-ph/0507047].

[40] A.V. Kotikov, Phys. Lett. B **254** (1991) 158; Phys. Lett. B **259** (1991) 314; Phys. Lett. B **267** (1991) 123;
E. Remiddi, Nuovo Cim. A **110** (1997) 1435. [hep-th/9711188];
M. Caffo, H. Czyz, S. Laporta and E. Remiddi, Acta Phys. Polon. B **29** (1998) 2627; [hep-th/9807119]; Nuovo Cim. A **111** (1998) 365. [hep-th/9805118];
T. Gehrmann and E. Remiddi, Nucl. Phys. B **580** (2000) 485 [hep-ph/9912329];
M. Argeri and P. Mastrolia, Int. J. Mod. Phys. A **22** (2007) 4375 [arXiv:0707.4037].

[41] C. Anastasiou and A. Lazopoulos, JHEP **0407** (2004) 046 [hep-ph/0404258].

[42] J. Gluza, K. Kajda and T. Riemann, Comput. Phys. Commun. **177** (2007) 879 [arXiv:0704.2423].

[43] M. Czakon, Comput. Phys. Commun. **175** (2006) 559 [hep-ph/0511200].

[44] A B. Goncharov, Math. Res. Lett. 5 (1998), 497-516.
D.J. Broadhurst, Eur. Phys. J. C **8** (1999) 311 [hep-th/9803091].
E. Remiddi and J.A.M. Vermaseren, Int. J. Mod. Phys. A **15** (2000) 725 [hep-ph/9905237].
T. Gehrmann and E. Remiddi, Comput. Phys. Commun. **141** (2001) 296 [hep-ph/0107173].
J. Vollinga and S. Weinzierl, Comput. Phys. Commun. **167** (2005) 177 [hep-ph/0410259].
D. Maître, Comput. Phys. Commun. **174** (2006) 222 [hep-ph/0507152]. hep-ph/0703052.

[45] T. Gehrmann and E. Remiddi, Nucl. Phys. B **601** (2001) 248 [hep-ph/0008287]; Nucl. Phys. B **601** (2001) 287 [hep-ph/0101124]; Comput. Phys. Commun. **144** (2002) 200 [hep-ph/0111255].

[46] K. Melnikov and T. van Ritbergen, Nucl. Phys. B **591** (2000) 515 [hep-ph/0005131].

[47] G. Heinrich, Nucl. Phys. Proc. Suppl. **116** (2003) 368 [hep-ph/0211144];
A. Gehrmann-De Ridder, T. Gehrmann and G. Heinrich, Nucl. Phys. B **682** (2004) 265 [hep-ph/0311276];
C. Anastasiou, K. Melnikov and F. Petriello, Phys. Rev. D **69** (2004) 076010 [hep-ph/0311311];
T. Binoth and G. Heinrich, Nucl. Phys. B **693** (2004) 134 [hep-ph/0402265];
G. Heinrich, Nucl. Phys. Proc. Suppl. **135** (2004) 290 [hep-ph/0406332]; Eur. Phys. J. C **48** (2006) 25 [hep-ph/0601062].

[48] D.A. Kosower, Phys. Rev. D **67** (2003) 116003 [hep-ph/0212097];
A. Gehrmann-De Ridder, T. Gehrmann and E.W.N. Glover, JHEP **0509** (2005) 056 [hep-ph/0505111];
A. Daleo, T. Gehrmann and D. Maître, JHEP **0704** (2007) 016 [hep-ph/0612257].

[49] S. Catani and M. Grazzini, Phys. Rev. Lett. **98** (2007) 222002 [hep-ph/0703012].

[50] C. Anastasiou, K. Melnikov and F. Petriello, Phys. Rev. Lett. **93** (2004) 262002 [hep-ph/0409088]; Nucl. Phys. B **724** (2005) 197 [hep-ph/0501130]; JHEP **0709** (2007) 014 [hep-ph/0505069];
K. Melnikov and F. Petriello, Phys. Rev. Lett. **96** (2006) 231803 [hep-ph/0603182]; Phys. Rev. D **74** (2006) 114017 [hep-ph/0609070];
C. Anastasiou, G. Dissertori and F. Stöckli, JHEP **0709** (2007) 018 [arXiv:0707.2373].

[51] A. Gehrmann-De Ridder, T. Gehrmann, E.W.N. Glover and G. Heinrich, Phys. Rev. Lett. **99** (2007) 132002 [arXiv:0707.1285]; JHEP **0711** (2007) 058 [arXiv:0710.0346]; JHEP **0712** (2007) 094 [arXiv:0711.4711]; Phys. Rev. Lett. **100** (2008) 172001 [arXiv:0802.0813].

[52] M. Grazzini, JHEP **0802** (2008) 043 [arXiv:0801.3232].